SCIENTIFIC REPORTS
nature research

OPEN

Light scattering effect of polyvinyl-alcohol/titanium dioxide nanofibers in the dye-sensitized solar cell

Muhammad Norhaffis Mustafa[1], Suhaidi Shafie[2,3], Mohd Haniff Wahid[1] & Yusran Sulaiman[1,3*]

In the present work, polyvinyl-alcohol/titanium dioxide (PVA/TiO_2) nanofibers are utilized as a light scattering layer (LSL) on top of the TiO_2 nanoparticles photoanode. The TiO_2 nanoparticles decorated PVA/TiO_2 nanofibers display a power conversion efficiency (PCE) of 4.06%, which is 33% higher than TiO_2 nanoparticles without LSL, demonstrating the incorporation of PVA/TiO_2 nanofibers as LSL reduces the radiation loss and increases the excitation of the electron that leads to high PCE. The incorporation of PVA/TiO_2 nanofibers as LSL also increases the electron life time and charge collection efficiency in comparison to the TiO_2 nanoparticles without LSL.

In dye-sensitized solar cells (DSSCs), light scattering layer (LSL) is important to prevent or reduce the amount of light loss during the DSSC process that could lead to reducing in power conversion efficiency (PCE). In the DSSC process, the higher the amount of light trapped on the sensitized photoanode, the more dye molecules will be excited and more voltage and current will be produced, resulting in an increase of PCE of the DSSC device[1]. Usami[2] reported a theoretical concept of light scattering layer by introducing larger TiO_2 nanoparticles on top of the TiO_2 photoanode to increase the light scattering and to improve the optical absorption of the photoanodes. Figure 1 shows the illustration of light loss of the photoanode with and without LSL.

A lot of one-dimensional TiO_2 morphological structures have been studied as LSL in DSSC such as nanofibers[3–5], nanorods[6] and nanotubes[7] because they can provide a straight pathway for the electron transfer and improve the electron transport rate to reduce the recombination effect significantly[8–10]. Among those one-dimensional structures, TiO_2 nanofibers are one of the most attractive one-dimensional nanostructure materials for LSL in DSSC because of their unique properties such as high surface area-to-volume ratio[11] and porous structure[12,13]. Furthermore, nanofibers can be synthesized from various materials, such as natural polymers[14], synthetic polymers[15], carbon-based nanomaterials[16,17], composite materials[18,19] and semiconducting materials[20]. Zheng and Zhu[21] reported that LSL made of gold doped TiO_2 nanofibers via electrospinning capable of producing a PCE of 5.08% due to an increase in the light harvesting efficiency. Furthermore, cadmium doped TiO_2 nanofibers as LSL in DSSC were successfully prepared by Motlak, *et al.*[22] via electrospinning. A PCE of 2.95% was achieved which is higher than bare photoanode (1.54%) due to the increase in the density of the electrons and increase in the injected electrons in the photoanode with LSL that leads to increase electron lifespan and preventing electron-holes recombination. A mixed phase of copper oxide nanoparticles ($CuO\text{-}Cu_2O$) prepared by microwave heating technique was used as LSL in DSSC and a higher PCE of 2.31% was achieved compared with pure DSSC without LSL (1.76%)[23]. This is due to the increase in dye loading capacity and improve light scattering ability[23].

Herein, we introduce a facile electrospinning to prepare the PVA/TiO_2 nanofibers as LSL. The TiO_2 nanoparticles with PVA/TiO_2 nanofibers as LSL exhibited a higher dye loading capacity and a better DSSC performance compared with TiO_2 nanoparticles without LSL. Furthermore, the TiO_2 nanoparticles with PVA/TiO_2 nanofibers as LSL displayed a longer electron life time and higher charge collection efficiency compared with TiO_2 nanoparticles without LSL.

Experimental

Materials. Ruthenizer 535-bis TBA (N719) and Iodolyte Z-100 were purchased from Solaronix SA while, 3,4-ethylenedioxythiophene (EDOT), titanium tetraisopropoxide (TTIP), polyvinyl alcohol (PVA) and titanium dioxide (TiO_2, Degussa P25) were purchased from Sigma Aldrich. Tert-butanol ($C_4H_{10}O$), ethanol (CH_3CH_2OH),

[1]Department of Chemistry, Faculty of Science, Universiti Putra Malaysia, 43400, Serdang, Selangor, Malaysia. [2]Department of Electrical and Electronics Engineering, Faculty of Engineering, Universiti Putra Malaysia, 43400 UPM, Serdang, Selangor, Malaysia. [3]Functional Devices Laboratory, Institute of Advanced Technology, Universiti Putra Malaysia, 43400 UPM, Serdang, Selangor, Malaysia. *email: yusran@upm.edu.my

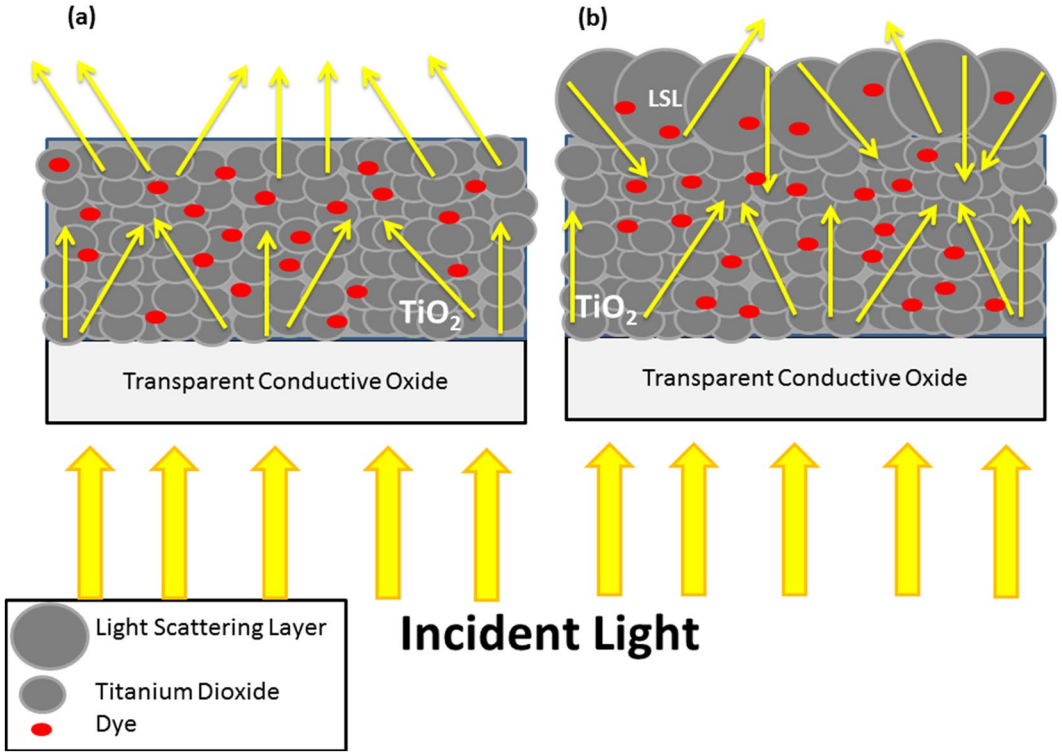

Figure 1. Illustration of light loss of (**a**) photoanode without light scattering layer and (**b**) photoanode with light scattering layer.

sodium hydroxide (NaOH), nanocrystalline cellulose (NCC) and acetonitrile were obtained from Merck, J. Kollin Chemicals, University of Maine and Friendemann Schmidt, respectively. Indium tin oxide (ITO 7Ω/sq) was purchased from Xinyan Technology Ltd. Deionized (DI) water (Mili-Q 18.2 MΩ.cm) was used throughout the experiments.

Preparation of photoanodes. The TiO_2 photoanodes were prepared using a doctor blade technique. Briefly, the TiO_2 pastes were prepared by mixing 8 mL of ethanol with 2 g of TiO_2 (Degussa P25). The mixture was stirred and 0.16 mL of TTIP was added into the mixture followed by sonication in an ultrasonic bath for 30 minutes. A TiO_2 compact layer was deposited on the ITO as previously reported[24]. The doctor blade technique was then applied to deposit the TiO_2 paste on the ITO/compact layer. The ITO/compact layer/TiO_2 photoanodes were annealed at 200 °C for two hours using a hot plate. The photoanodes were then immersed in a dye bath solution containing 0.2 mM (N719) in the same ratio of acetonitrile and tert-butanol for 24 hours to produce sensitized photoanodes.

Preparation of PVA/TiO_2 nanofibers as a light scattering layer. The light scattering layer was prepared using electrospinning. 10 wt.% of PVA was dissolved in DI water and stirred at 80 °C until a clear PVA solution was formed. 0.06 M TTIP was then added into the PVA solution and stirred for 2 hours to form the electrospun solution. The as-prepared electrospun solution was transferred into a 5 mL syringe with a blunt needle. The electrospinning was performed by applying a voltage of 15 kV and the flow rate of 1.2 mL/h. The distance between the tip of the needle and the current collector was fixed to 15 cm. The current collector was the as-prepared ITO/compact layer/TiO_2 photoanodes. The electrospun time to produce PVA/TiO_2 nanofibers was fixed to 9.88 min[25].

Preparation of counter electrode. The counter electrode for the DSSC was fabricated using a previously reported chronoamperometry technique[26]. Briefly, the PEDOT/NCC counter electrode was electrodeposited on the ITO using three electrode systems where the applied voltage and deposition time used were 1.2 V and 100 s, respectively. The electrodeposited solution consisted of 1 mg/mL NCC and 10 mM EDOT. The working, counter and reference electrode used were ITO, platinum wire and silver/silver chloride, respectively.

Device fabrication. A complete DSSC device was assembled by sandwiching both the sensitized photoanodes (ITO/compact layer/TiO_2/LSL) and counter electrode (PEDOT/NCC). The electrolyte (Iodolyte Z-100) was injected in between the photoanodes and counter electrode. A black mask with an active area of 0.25 cm^2 was used to analyze the DSSC performance.

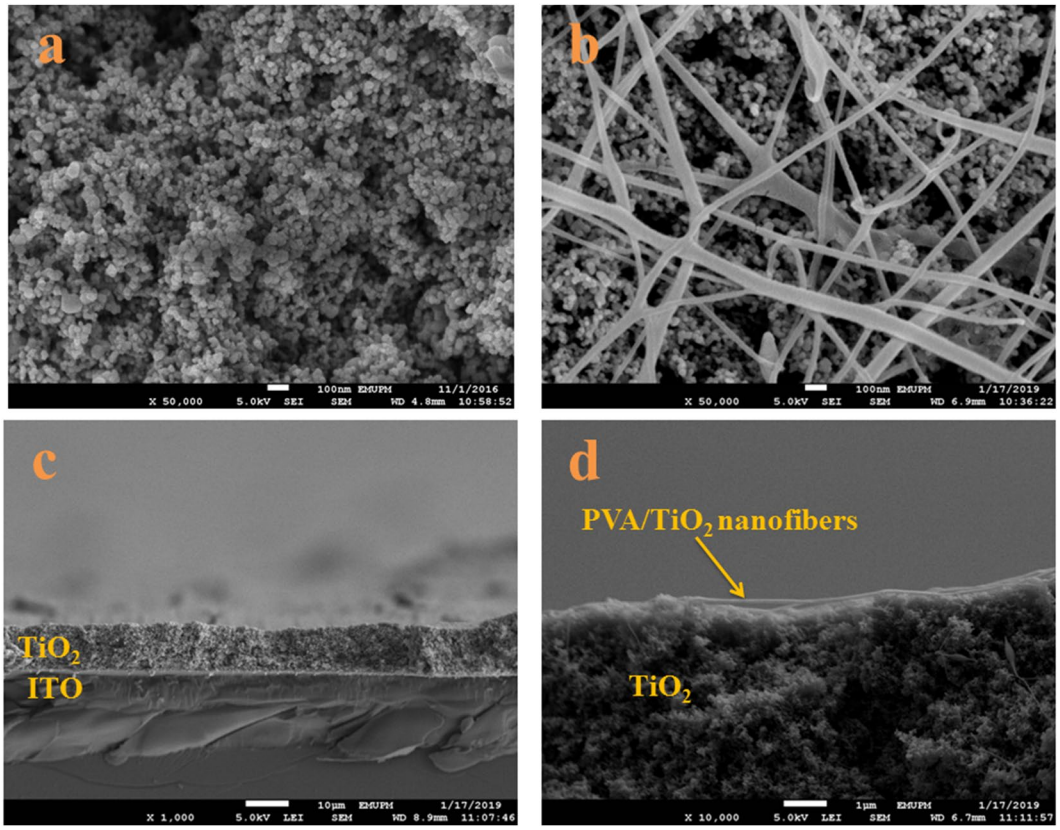

Figure 2. FESEM image of (**a**) TiO_2 nanoparticles, (**b**) TiO_2 nanoparticles with PVA/TiO_2 nanofibers, (**c**) cross-sectional of TiO_2 nanoparticle (**d**) cross-sectional of TiO_2 nanoparticles with PVA/TiO_2 nanofibers.

Characterization. The morphological studied was performed using the field emission scanning electron microscopy (FESEM, JEOL JSM-7600F). The crystallographic analysis of the photoanodes was performed using Shimadzu X-ray diffraction (XRD) Diffractometer with Cu Kα radiation ($\lambda = 1.54$ Å). The electrochemical impedance spectroscopy (EIS) was carried out using Autolab PGSTAT204 equipped with NOVA software. The EIS was carried out in a dark condition at open circuit potential (OCP) of 0.8 V and a frequency range between 100 kHz to 1 Hz in the presence of Iodolyte Z-100. The dye loading capacity analysis of the photoanodes was performed using Autolab Spectrophotometer UB in the range of 200–550 nm. The sensitized photoanodes were immersed into 0.1 M NaOH solution to desorb the dye (N719) molecules from the photoanodes and the solutions were tested with ultraviolet-visible (UV-Vis) analysis to calculate the amount of the dye (N719) molecules absorbed by the photoanodes. The photovoltaic analysis of the complete DSSC devices was performed using Oriel LCS-100 solar stimulator (1.5 A.M, 100 mW/cm^2 and 100 watt Xenon lamp) equipped with a potentiostat (Autolab PGSTAT204).

Results and Discussion

Morphological studies. FESEM was performed to study the morphology of the photoanode. Figure 2 shows the FESEM images of TiO_2 nanoparticles and TiO_2 nanoparticles with the PVA/TiO_2 nanofibers. Figure 2a depicts the spherical nanoparticles structure of TiO_2 which is important in the absorption of the dye. As shown in Fig. 2b, the TiO_2 nanoparticles with PVA/TiO_2 nanofibers display a network of fibers that cover the surface of spherical nanoparticles of TiO_2 with an average diameter of 45 ± 20 nm. The large diameter of PVA/TiO_2 nanofibers than TiO_2 spherical nanoparticles is important to create a light scattering effect to trap the sunlight and increase the PCE of the DSSC[27]. The cross-sectional of TiO_2 nanoparticles and TiO_2 nanoparticles with PVA/TiO_2 nanofibers are shown in Fig. 2c,d, respectively. The results illustrate that the PVA/TiO_2 nanofibers is thinner than TiO_2 nanoparticles and only cover the top of TiO_2 nanoparticles. A thin LSL is important to avoid the increase in the internal resistance that will reduce the DSSC performance[28].

X-ray diffraction analysis. XRD was performed to study the crystalline structure of the photoanodes. Figure 3 shows the XRD patterns of PVA, TiO_2 nanoparticles, TiO_2 nanoparticles with PVA/TiO_2 nanofibers and PVA/TiO_2 nanofibers. All the diffraction peaks of TiO_2 nanoparticles can be well indexed to the anatase and rutile phase of TiO_2 (JCPDS 01-073-1764) and the same XRD patterns were reported by Zhao, *et al.*[29]. The diffraction peak of PVA appears at around $2\theta = 22°$ (101)[30]. PVA/TiO_2 nanofibers displays all the peak belongs to PVA and TiO_2. Upon addition of PVA/TiO_2 nanofibers, one additional characteristic peak at around $2\theta = 22°$ (101) is observed, indicating the presence of PVA[30].

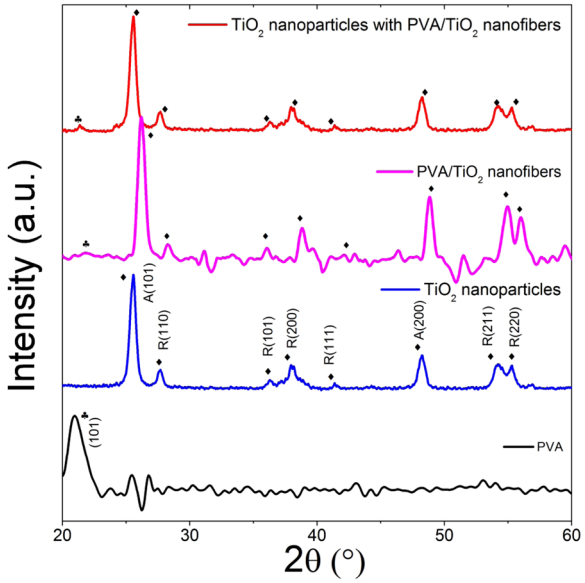

Figure 3. XRD pattern of TiO_2 nanoparticles, TiO_2 nanoparticles with PVA/TiO_2 nanofibers and PVA/TiO_2 nanofibers. Peaks labeled with "♦" and "♣" belong to the peaks of TiO_2 and PVA, respectively.

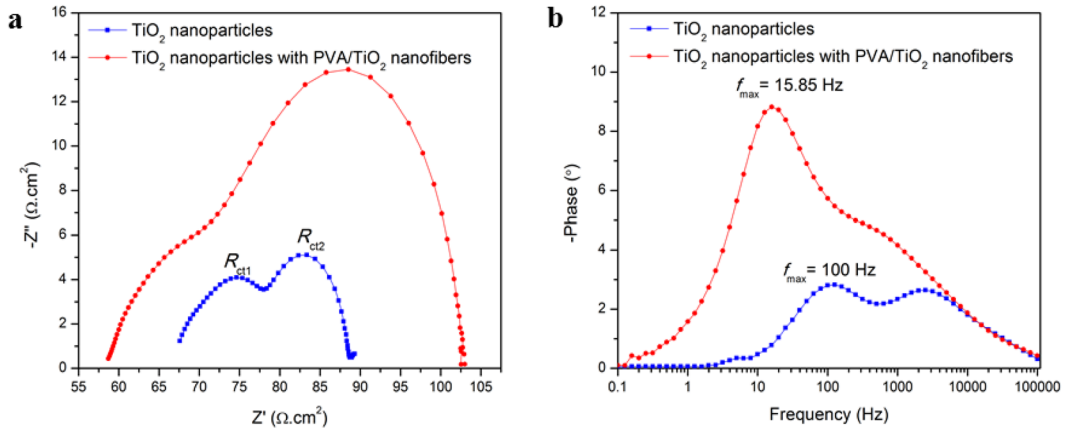

Figure 4. (**a**) Nyquist plot and (**b**) bode plot of TiO_2 nanoparticles and TiO_2 nanoparticles with PVA/TiO_2 nanofibers.

Photoanodes	R_s (Ω.cm²)	R_{ct1} (Ω.cm²)	R_{ct2} (Ω.cm²)	f_{max} (Hz)	τ_n (ms)	η_c (%)
TiO_2 nanoparticles	67.60	17.00	12.70	100.0	1.59	15.8
TiO_2 nanoparticles with PVA/TiO_2 nanofibers	58.34	29.25	34.03	15.85	10.04	36.84

Table 1. EIS parameter of the DSSCs based on TiO_2 nanoparticles and TiO_2 nanoparticles with PVA/TiO_2 nanofibers.

Electrochemical impedance spectroscopy. Figure 4a displays a comparison of Nyquist plots between TiO_2 nanoparticles and TiO_2 nanoparticles with PVA/TiO_2 nanofibers. Two semicircles are clearly observed: the high frequency semicircle (R_{ct1}) corresponds to the charge transfer resistance at the counter electrode interface, while the low frequency semicircle (R_{ct2}) is attributed to the charge transfer resistance at TiO_2/dye/electrolyte interface[31]. Upon addition of PVA/TiO_2 nanofibers as LSL on top of TiO_2 nanoparticles, the R_{ct1} increases (Table 1) due to the presence of a new layer on top of the photoanode obstructs the movement of the electron to complete the electron-regeneration process[32]. Furthermore, TiO_2 nanoparticles with PVA/TiO_2 nanofibers displays a higher R_{ct2} (34.03 Ω.cm²) compared to the R_{ct2} of TiO_2 nanoparticles (12.70 Ω.cm²) (Table 1). This is because the addition of PVA/TiO_2 nanofibers as LSL on top of the TiO_2 nanoparticles will increase the resistance at the TiO_2/dye/electrolyte interface[28,33]. However, TiO_2 nanoparticles with PVA/TiO_2 nanofibers depicts a lower series resistance (R_s) of 58.34 Ω.cm² compared with TiO_2 nanoparticles (67.60 Ω.cm²), demonstrating the

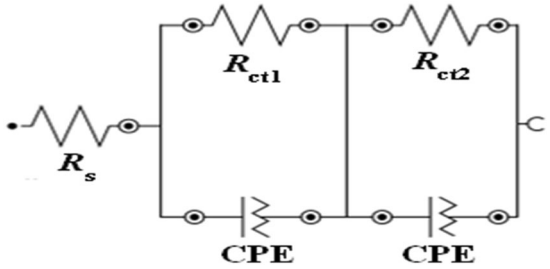

Figure 5. Equivalent circuit for EIS.

incorporation of PVA/TiO_2 nanofibers as LSL slightly increases the conductivity of the photoanode. This fact is supported by the conductive TiO_2 was well blended with PVA nanofibers during electrospinning. Apart from charge transfer resistance, the charge collection efficiency (η_c) also can be calculated from EIS analysis using formula 1[34]. TiO_2 nanoparticles with PVA/TiO_2 nanofibers displays a higher η_c (38.84%) compared with TiO_2 nanoparticles (15.8%), indicating that incorporation of PVA/TiO_2 nanofibers as LSL improves the light scattering effect of the photoanodes that lead to increase in η_c.

$$\eta_c = \left(1 + \frac{R_s}{R_{ct2}}\right)^{-1} \quad (1)$$

As shown in Fig. 4b, Bode plot analysis was extracted from EIS analysis to study the electron life time (τ_n) between TiO_2 nanoparticles and TiO_2 nanoparticles with PVA/TiO_2 nanofibers. The f_{max} value of TiO_2 nanoparticles and TiO_2 nanoparticles with PVA/TiO_2 nanofibers are 100 and 15.85 Hz while the τ_n values of TiO_2 nanoparticles and TiO_2 nanoparticles with PVA/TiO_2 nanofibers are 1.59 and 10.04 ms, respectively (Table 1). The τ_n values of TiO_2 nanoparticles and TiO_2 nanoparticles with PVA/TiO_2 nanofibers were calculated using formula 2[34].

$$\tau_n = \frac{1}{2\pi f_{max}} \quad (2)$$

Upon incorporation of PVA/TiO_2 nanofibers as LSL, the maximum frequency (f_{max}) is shifted from a higher frequency region to lower frequency region, producing a longer τ_n and improves the light scattering capability of the photoanode. Figure 5 shows the electrical equivalent circuit that was constructed by fitting the EIS data. The fitting circuit models consist of R_s, R_{ct1}, R_{ct2} and constant phase element (CPE). The CPE indicates the inhomogeneity of the photoanode after being modified[35]. The low chi-square achieves by TiO_2 nanoparticles (0.00109) and TiO_2 nanoparticles with PVA/TiO_2 nanofibers (0.00011) indicate the better suitability of the equivalent circuit with the Nyquist plot.

Ultraviolet-visible analysis. The UV-Vis analysis was performed to study the dye loading capacity of photoanodes with and without LSL. Figure 6 displays the UV-Vis absorption spectra of TiO_2 nanoparticles and TiO_2 nanoparticles with PVA/TiO_2 nanofibers. Both UV-Vis spectra depict four main absorption peaks at wavelength 230, 307, 375 and 505 nm. The absorption peaks at lower energies (375 and 505 nm) are attributed to the metal-to-ligand charge transfer (MLCT) transition ($4d - \pi^*$) while the absorption peaks at higher energies (230 and 307 nm) are ascribed to the ligand-centered charge transfer (LCCT) transitions ($\pi - \pi^*$)[36]. TiO_2 nanoparticles with PVA/TiO_2 nanofibers displays higher absorption peaks compared to the TiO_2 nanoparticles, indicating that the incorporation of PVA/TiO_2 nanofibers as LSL increases the dye loading capacity of the photoanodes. The amounts of dye molecules absorbed by TiO_2 nanoparticles and TiO_2 nanoparticles with PVA/TiO_2 nanofibers are 0.035 and 0.037 mmol cm^{-2}, respectively. The increment in the concentration of dye molecules absorbed by the photoanode with LSL is due to the morphological structure of PVA/TiO_2 nanofibers that increase the surface area of the photoanode, resulting to more dye molecules can be absorbed by the photoanode.

Photovoltaic performance of the DSSCs. Dark current-voltage (J-V) curve analysis was performed to investigate the back electron transfer process in DSSC. Figure 7a shows the dark J-V curve of TiO_2 nanoparticles and TiO_2 nanoparticles with PVA/TiO_2 nanofibers. The onset of the dark currents for TiO_2 nanoparticles and TiO_2 nanoparticles with PVA/TiO_2 nanofibers occur at around 0.58 and 0.62 V, indicating reduce in back electron transfer for a latter compared to a former photoanode. J-V curves were performed under 1 sun illumination with A.M 1.5 G to investigate the total PCE generated by TiO_2 nanoparticles and TiO_2 nanoparticles with PVA/TiO_2 nanofibers. As shown in Fig. 7b, the TiO_2 nanoparticles with PVA/TiO_2 nanofibers display a higher PCE of 4.09% compared to the TiO_2 nanoparticles (3.06%). Figure 7c shows that upon addition of PVA/TiO_2 nanofibers as LSL on the photoanode, the maximum power generated by the DSSC increases. Table 2 summarizes and compares the photovoltaic performance of the DSSC devices. The photoanode with LSL shows a vast increment of PCE which about 33% more than the photoanode without LSL, indicating the incorporation of PVA/TiO_2 nanofibers as LSL improves the current and voltage generated throughout the DSSC process that leads to high PCE produces. This fact is supported by the increment of both short circuit current density (J_{sc}) and open circuit voltage (V_{oc}) of photoanode with PVA/TiO_2 nanofibers as LSL compared to the photoanode without LSL. The increment of both J_{sc}

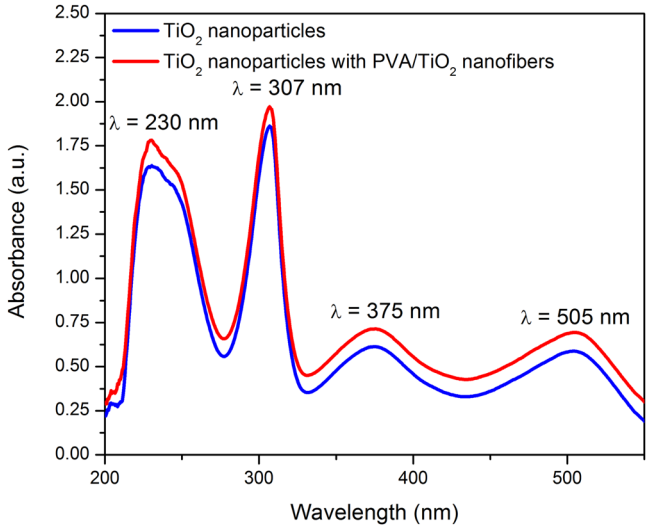

Figure 6. UV-Vis absorption of TiO_2 nanoparticles and TiO_2 nanoparticles with PVA/TiO_2 nanofibers.

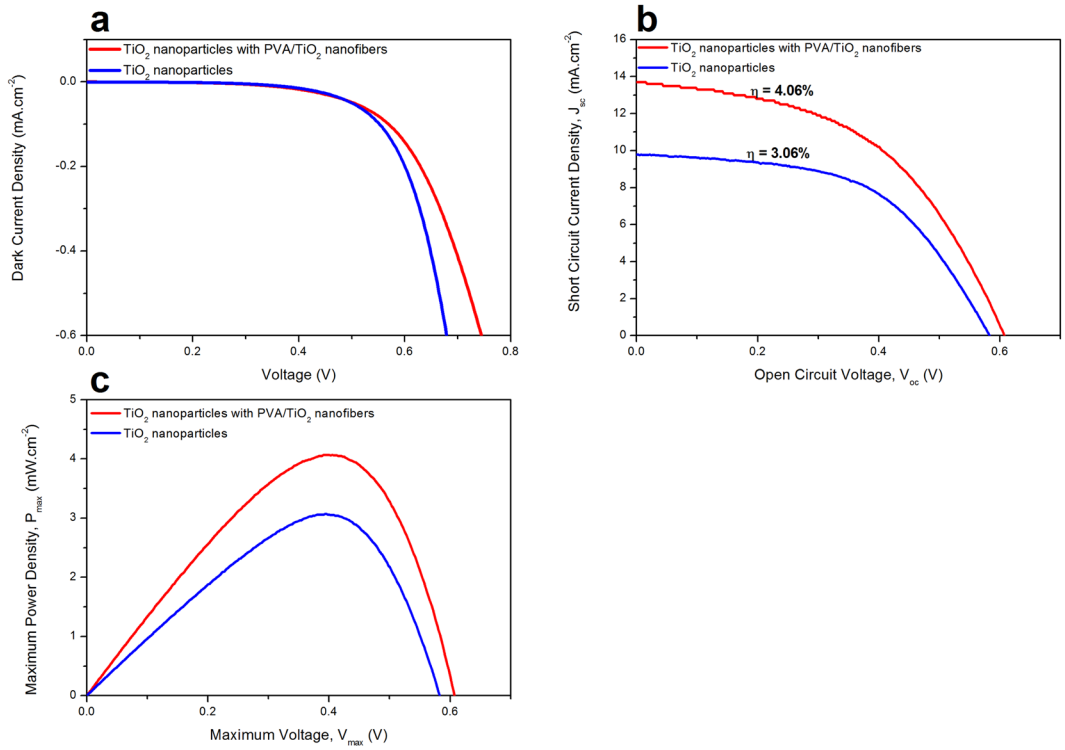

Figure 7. (**a**) Dark J-V curve, (**b**) J-V curve under illumination and (**c**) P-V curve of TiO_2 nanoparticles and TiO_2 nanoparticles with PVA/TiO_2 nanofibers.

and V_{oc} after incorporation of LSL demonstrates that the LSL help to reduce the radiation loss during DSSC process[27,28]. This extra radiation helps to excite more electrons of the dye molecules, producing more electron-hole junction that leads to more power to be generated. As a consequence, the maximum voltage and maximum power of the DSSC device with PVA/TiO_2 nanofibers as LSL increases. Even though the total PCE of the DSSC device with PVA/TiO_2 nanofibers as LSL improves compared with the DSSC device without LSL, the fill factor undergo a slight drop from 53.89 to 48.58% due to the addition of LSL increases the internal resistant of photoanode[28]. This result is in agreement with the EIS analysis where an increase in R_{ct} is observed upon addition of PVA/TiO_2 nanofibers as LSL. The PCE obtained in this study is comparable with the cadmium doped TiO_2 nanofibers (2.95%)[22], sulfur doped TiO_2 nanofibers (4.27%)[37] and gold doped TiO_2 nanofibers (5.08%)[21].

Photoanodes	J_{sc} (mA/cm²)	V_{oc} (V)	P_{max} (mW/cm²)	FF (%)	η (%)	References
Cadmium doped TiO_2 nanofibers	8.73	0.68	2.73	46.20	2.95	[22]
Sulfur doped TiO_2 nanofibers	10.66	0.68	4.27	59.00	4.27	[37]
Gold doped TiO_2 nanofibers	10.07	0.76	5.08	76.00	5.08	[21]
TiO_2 nanoparticles with PVA/TiO_2 nanofibers	13.70	0.61	4.06	48.58	4.06	This work

Table 2. Comparison of the Photovoltaic performances of the DSSCs.

Conclusion

TiO_2 nanoparticles decorated with PVA/TiO_2 nanofibers as LSL with remarkably enhanced DSSC performance were successfully synthesized. The PVA/TiO_2 nanofibers were prepared by facile electrospinning using PVA as a polymer source and TTIP as conductive metal oxide precursor. Upon addition of the PVA/TiO_2 nanofibers as LSL on top of the photoanode, the PCE of the DSSC device increased 33% compared to the photoanode without LSL. This outstanding enhancement of PCE was attributed to the fact that the LSL reduced the radiation loss, producing more oxidation of dye molecule, resulting in more electrons to be excited and more PCE to be generated.

Received: 19 June 2019; Accepted: 9 September 2019;

Published online: 18 October 2019

References

1. Zhu, P. *et al*. Mesoporous SnO_2 agglomerates with hierarchical structures as an efficient dual-functional material for dye-sensitized solar cells. *Chemical Communications* **48**, 10865–10867, https://doi.org/10.1039/C2CC36049G (2012).
2. Usami, A. Theoretical study of application of multiple scattering of light to a dye-sensitized nanocrystalline photoelectrichemical cell. *Chemical Physics Letters* **277**, 105–108, https://doi.org/10.1016/S0009-2614(97)00878-6 (1997).
3. Joshi, P. *et al*. Composite of TiO_2 nanofibers and nanoparticles for dye-sensitized solar cells with significantly improved efficiency. *Energy & Environmental Science* **3**, 1507–1510, https://doi.org/10.1039/C0EE00068J (2010).
4. Kokubo, H., Ding, B., Naka, T., Tsuchihira, H. & Shiratori, S. Multi-core cable-like TiO_2 nanofibrous membranes for dye-sensitized solar cells. *Nanotechnology* **18**, 165604, https://doi.org/10.1088/0957-4484/18/16/165604 (2007).
5. Dong, Z., Kennedy, S. J. & Wu, Y. Electrospinning materials for energy-related applications and devices. *Journal of Power Sources* **196**, 4886–4904, https://doi.org/10.1016/j.jpowsour.2011.01.090 (2011).
6. Jiu, J., Isoda, S., Wang, F. & Adachi, M. Dye-Sensitized Solar Cells Based on a Single-Crystalline TiO_2 Nanorod Film. *The Journal of Physical Chemistry B* **110**, 2087–2092, https://doi.org/10.1021/jp055824n (2006).
7. Lin, C.-J., Yu, W.-Y. & Chien, S.-H. Rough conical-shaped TiO_2-nanotube arrays for flexible backilluminated dye-sensitized solar cells. *Applied Physics Letters* **93**, 133107, https://doi.org/10.1063/1.2992585 (2008).
8. Liu, B. & Aydil, E. S. Growth of Oriented Single-Crystalline Rutile TiO_2 Nanorods on Transparent Conducting Substrates for Dye-Sensitized Solar Cells. *Journal of the American Chemical Society* **131**, 3985–3990, https://doi.org/10.1021/ja8078972 (2009).
9. Yang, L. & Leung, W. W.-F. Application of a Bilayer TiO_2 Nanofiber Photoanode for Optimization of Dye-Sensitized Solar Cells. *Advanced Materials* **23**, 4559–4562, https://doi.org/10.1002/adma.201102717 (2011).
10. Rui, Y. *et al*. Template-free synthesis of hierarchical TiO_2 hollow microspheres as scattering layer for dye-sensitized solar cells. *Applied Surface Science* **369**, 170–177, https://doi.org/10.1016/j.apsusc.2016.02.049 (2016).
11. Peng, S. *et al*. Multi-functional electrospun nanofibres for advances in tissue regeneration, energy conversion & storage, and water treatment. *Chemical Society reviews* **45**, 1225–1241, https://doi.org/10.1039/C5CS00777A (2016).
12. Kenry & Lim, C. T. Nanofiber technology: current status and emerging developments. *Progress in Polymer Science* **70**, 1–17, https://doi.org/10.1016/j.progpolymsci.2017.03.002 (2017).
13. Lee, J. K. Y. *et al*. Polymer-based composites by electrospinning: Preparation & functionalization with nanocarbons. *Progress in Polymer Science* **86**, 40–84, https://doi.org/10.1016/j.progpolymsci.2018.07.002 (2018).
14. Hassanzadeh, P. *et al*. Chitin nanofiber micropatterned flexible substrates for tissue engineering. *Journal of Materials Chemistry B* **1**, 4217–4224, https://doi.org/10.1039/C3TB20782J (2013).
15. Behrens, A. M. *et al*. *In Situ* Deposition of PLGA Nanofibers via Solution Blow Spinning. *ACS Macro Letters* **3**, 249–254, https://doi.org/10.1021/mz500049x (2014).
16. Yang, X. *et al*. Activated nitrogen-doped carbon nanofibers with hierarchical pore as efficient oxygen reduction reaction catalyst for microbial fuel cells. *Journal of Power Sources* **266**, 36–42, https://doi.org/10.1016/j.jpowsour.2014.04.126 (2014).
17. Ji, D. *et al*. Design of 3-Dimensional Hierarchical Architectures of Carbon and Highly Active Transition Metals (Fe, Co, Ni) as Bifunctional Oxygen Catalysts for Hybrid Lithium–Air Batteries. *Chemistry of Materials* **29**, 1665–1675, https://doi.org/10.1021/acs.chemmater.6b05056 (2017).
18. Wu, Q., Tran, T., Lu, W. & Wu, J. Electrospun silicon/carbon/titanium oxide composite nanofibers for lithium ion batteries. *Journal of Power Sources* **258**, 39–45, https://doi.org/10.1016/j.jpowsour.2014.02.047 (2014).
19. Ji, D. *et al*. Atomically Transition Metals on Self-Supported Porous Carbon Flake Arrays as Binder-Free Air Cathode for Wearable Zinc-Air Batteries. *Advanced Materials* **31**, 1808267, https://doi.org/10.1002/adma.201808267 (2019).
20. Shang, M. *et al*. The design and realization of a large-area flexible nanofiber-based mat for pollutant degradation: an application in photocatalysis. *Nanoscale* **5**, 5036–5042, https://doi.org/10.1039/C3NR00503H (2013).
21. Zheng, F. & Zhu, Z. Preparation of the Au@TiO_2 nanofibers by one-step electrospinning for the composite photoanode of dye-sensitized solar cells. *Materials Chemistry and Physics* **208**, 35–40, https://doi.org/10.1016/j.matchemphys.2018.01.021 (2018).
22. Motlak, M., Hamza, A. M., Hammed, M. G. & Barakat, N. A. M. Cd-doped TiO_2 nanofibers as effective working electrode for the dye sensitized solar cells. *Materials Letters* **246**, 206–209, https://doi.org/10.1016/j.matlet.2019.03.067 (2019).
23. Wongratanaphisan, D. *et al*. CuO-Cu_2O nanocomposite layer for light-harvesting enhancement in ZnO dye-sensitized solar cells. *Applied Surface Science* **474**, 85–90, https://doi.org/10.1016/j.apsusc.2018.05.037 (2019).
24. Mustafa, M. N., Shafie, S., Wahid, M. H. & Sulaiman, Y. Optimization of power conversion efficiency of polyvinyl-alcohol/titanium dioxide compact layer using response surface methodology/central composite design. *Sol. Energy* **183**, 689–696, https://doi.org/10.1016/j.solener.2019.03.074 (2019).
25. Mustafa, M. N., Shafie, S., Wahid, M. H. & Sulaiman, Y. Optimization of power conversion efficiency of polyvinyl-alcohol/titanium dioxide as light scattering layer in DSSC using response surface methodology/central composite design. *Results in Physics* **15**, 102559, https://doi.org/10.1016/j.rinp.2019.102559 (2019).

26. Mustafa, M. N., Shafie, S., Zainal, Z. & Sulaiman, Y. Poly(3,4-ethylenedioxythiophene) doped with various carbon-based materials as counter electrodes for dye sensitized solar cells. *Materials & Design* **136**, 249–257, https://doi.org/10.1016/j.matdes.2017.09.053 (2017).
27. Gong, J., Sumathy, K., Qiao, Q. & Zhou, Z. Review on dye-sensitized solar cells (DSSCs): Advanced techniques and research trends. *Renewable Sustainable Energy Rev.* **68**, 234–246, https://doi.org/10.1016/j.rser.2016.09.097 (2017).
28. Deepak, T. G. *et al*. A review on materials for light scattering in dye-sensitized solar cells. *RSC Adv.* **4**, 17615–17638, https://doi.org/10.1039/C4RA01308E (2014).
29. Zhao, A. *et al*. *Molecular interaction of fibrinogen with thermally modified titanium dioxide nanoparticles*. Vol. 4 (2014).
30. Ricciardi, R., Auriemma, F., De Rosa, C. & Lauprêtre, F. X-ray Diffraction Analysis of Poly(vinyl alcohol) Hydrogels, Obtained by Freezing and Thawing Techniques. *Macromolecules* **37**, 1921–1927, https://doi.org/10.1021/ma035663q (2004).
31. Lin, L.-Y., Lee, C.-P., Vittal, R. & Ho, K.-C. Improving the durability of dye-sensitized solar cells through back illumination. *Journal of Power Sources* **196**, 1671–1676, https://doi.org/10.1016/j.jpowsour.2010.08.032 (2011).
32. Ho, P., Bao, L. Q., Ahn, K.-S., Cheruku, R. & Kim, J. H. P-Type dye-sensitized solar cells: Enhanced performance with a NiO compact blocking layer. *Synthetic Metals* **217**, 314–321, https://doi.org/10.1016/j.synthmet.2016.04.006 (2016).
33. Zhang, Q., Myers, D., Lan, J., Jenekhe, S. A. & Cao, G. Applications of light scattering in dye-sensitized solar cells. *Phys. Chem. Chem. Phys.* **14**, 14982–14998, https://doi.org/10.1039/C2CP43089D (2012).
34. Lim, S. P., Pandikumar, A., Lim, H. N., Ramaraj, R. & Huang, N. M. Boosting Photovoltaic Performance of Dye-Sensitized Solar Cells Using Silver Nanoparticle-Decorated N,S-Co-Doped-TiO_2 Photoanode. *Scientific Reports* **5**, 11922, https://doi.org/10.1038/srep11922 (2015).
35. Azman, N. H. N., Lim, H. N., Mamat, M. S. & Sulaiman, Y. Synergistic Enhancement of Ternary Poly(3,4-ethylenedioxythiophene)/Graphene Oxide/Manganese Oxide Composite as a Symmetrical Electrode for Supercapacitors. *Energies* **11**, 1510 (2018).
36. Hirata, N. *et al*. Supramolecular control of charge-transfer dynamics on dye-sensitized nanocrystalline TiO_2 films. *Chemistry – A European Journal* **10**, 595–602, https://doi.org/10.1002/chem.200305408 (2004).
37. Mahmoud, M. S. *et al*. Demonstrated photons to electron activity of S-doped TiO_2 nanofibers as photoanode in the DSSC. *Materials Letters* **225**, 77–81, https://doi.org/10.1016/j.matlet.2018.04.108 (2018).

Acknowledgements

The authors appreciatively acknowledge the financial supports by the Universiti Putra Malaysia Research Grant (UPM/800-3/3/1/GPB/2018/9659200).

Author contributions

Y.S. supervised and coordinated the whole experiments. S.S. and M.H.W. co-supervised the whole experiments. M.N.M. performed the experiments, carried out the measurements, data analysis, reporting results and data interpretation. M.N.M. wrote the main manuscript.

Competing interests

The authors declare no competing interests.

Additional information

Correspondence and requests for materials should be addressed to Y.S.

Reprints and permissions information is available at www.nature.com/reprints.

Publisher's note Springer Nature remains neutral with regard to jurisdictional claims in published maps and institutional affiliations.